2009

Spin transfer torque switching of magnetic tunnel junctions using a conductive atomic force microscope

Erick R. Evarts
Carnegie Mellon University

Limin Cao
Carnegie Mellon University, limincao@andrew.cmu.edu

David S. Ricketts
Carnegie Mellon University, ricketts@andrew.cmu.edu

Nicholas D. Rizzo
Everspin Technologies

James A. Bain
Carnegie Mellon University, jbain@cmu.edu

See next page for additional authors

Published In
Appl. Phys. Lett. , 95, 132510.

Spin transfer torque switching of magnetic tunnel junctions using a conductive atomic force microscope

Eric R. Evarts,[1] Limin Cao,[2] David S. Ricketts,[2] Nicholas D. Rizzo,[3] James A. Bain,[2] and Sara A. Majetich[1,a)]
[1]*Department of Physics, Carnegie Mellon University, Pittsburgh, Pennsylvania 15213, USA*
[2]*Department of Electrical and Computer Engineering, Carnegie Mellon University, Pittsburgh, Pennsylvania 15213, USA*
[3]*Everspin Technologies, Inc., Chandler, Arizona 85224, USA*

(Received 8 August 2009; accepted 10 September 2009; published online 2 October 2009)

We show that a nonmagnetic conductive atomic force microscopy probe can be used to read and write magnetic bits using current passed between the tip and bit. The bits were patterned using electron beam lithography from a magnetic tunnel junction (MTJ) film with in-plane shape anisotropy using an MgO tunnel barrier. Probes were made having a thick Pt coating and could deliver up to several milliamps, so that MTJ structures were easily switched repeatedly using the spin transfer torque effect. © *2009 American Institute of Physics*. [doi:10.1063/1.3240884]

The ability to switch the magnetization of a nanomagnet using current has tremendous implications for data storage and logic applications. Early work on magnetization reversal using spin transfer torque (STT) studied effects in metallic spin-valve structures with resistance changes of milliohms;[1] however, the same effect with larger resistance changes has been observed in magnetic tunnel junction (MTJ) structures.[2] The devices in this previous work have used fixed leads for characterization, but fixed leads will present serious challenges if MTJs are to be used for data storage with several terabit per square inch data density.[3,4]

Other groups have previously investigated the use of scanning probes for information storage. The IBM Millipede project[5] with dense arrays of scanning probes used a thermomechanical approach to read and write bits with a special resistive heater probe to controllably deform a thin polymer film. However, this can only be changed a limited number of times and can only erase large areas at a time.[6] In other work, atomic force microscopy (AFM) has been used to mechanically deform surfaces[7] or to oxidize metals[8] to produce small patterns, but these techniques are not rewritable. Conductive AFM (CAFM) has been used to read and write polarization bits in polymers[9] and multiferroics,[10–13] but the lifetime of the recorded data is limited or the resistance/polarization changes over the timescale of a few days before settling into a more permanent value.

Current induced switching of iron nanoislands has been observed using spin-polarized scanning tunneling microscopy.[14] While these islands were not magnetically stable at room temperature, the use of scanning probes for reading and writing bits of information is an intriguing possibility. CAFM has previously been used to read the state of an MTJ before and after switching, but not to write it.[15] STT requires extremely high current densities ($\sim 10^6$–10^7 A/cm^2), which require much higher currents ($\sim$1 mA for 200×100 nm^2 pillars) than are common to scanning probe microscopy (approximately picoampere to approximately nanoampere for scanning tunneling microscopy (STM), $\sim$10 μA for CAFM).

Here we demonstrate how high current densities can be achieved in CAFM with nanopillar MTJs for reading using tunneling magnetoresistance and writing using STT, suggesting the possibility of a millipede-like system, where MTJ pillars share a common bottom electrode and are individually written and read with the probe. This geometry allows packing of bits at least as dense as in cross bar memory arrays, without the need of a separate selection device beneath each bit. The probe is the selection device.

The MTJ film fabricated by Everspin Technologies with an *RA* product of 6 ± 1 Ω μm^2 as measured with a current in plane probe tester (CIPT) was deposited as Si wafer $\sim$200 nm SiO_2\50 nm Ta\20 nm PtMn\2.0 nm CoFe\0.8 nm Ru\3.0 nm CoFe\1.0 nm MgO\2.5 nm CoFeB\8 nm Ta\10 nm Pt.[16] Pillars were defined using electron-beam lithography with MAN2403 negative resist and patterned by argon ion milling (500 V, 40 mA, 22.5° for 4.5 min) down to the Ta back electrode. The resist was then removed using oxygen plasma. The pillars were nominally rectangular in shape with sizes ranging from 1000×500 nm^2 down to 100×50 nm^2. A representative image is shown in Fig. 1. The long axis of the rectangles was aligned with the pinning direction of the antiferromagnet. The AFM topography indicated pillar heights of 60 nm, consistent with patterning through the whole magnetic stack.

Measurements were performed with a Veeco DI Dimension 3100 AFM with a signal access module. To support the high currents required for STT switching, commercial silicon probes with a nominal spring constant of 2.8 N/m were coated with a 200 nm Pt film by sputtering, which increases the tip radius to nominally 100 nm.[17] The increased coating thickness compared to commercial conductive probes combined with the larger contact area from the blunter tip to allow delivery of up to 10 mA before the coating melts or deforms appreciably. Electronic measurements were made using a Keithley model 2400 Sourcemeter in current sourcing mode with the positive electrode connected to the AFM tip, and the negative electrode connected to the Ta lower electrode. External in-plane magnetic fields were applied us-

a)Author to whom correspondence should be addressed. Electronic mail: sara@cmu.edu.

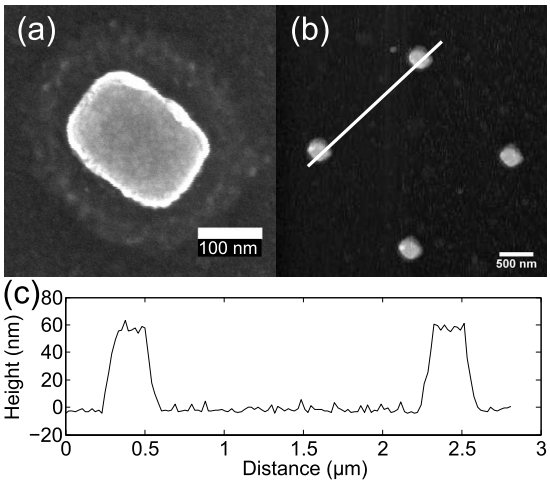

FIG. 1. (a) An SEM image of a 200×100 nm^2 patterned rectangular pillar. (b) AFM image of several pillars. (c) AFM topographic profile across two pillars indicated by the white line in (b). From the height shown in the AFM profile, we conclude that the pillars were patterned through the whole magnetic stack and into the bottom Ta electrode.

ing a custom quadrupole magnet with integrated Hall sensors capable of delivering a ±500 G field at the sample. The tip was stopped on top of a pillar, then a force of ~140 nN was applied to the tip to ensure proper electrical contact, and the tip was held in place until the electrical measurements were completed. The AFM used here had a mechanical drift of 5–10 nm/min, so measurements were performed in less than two minutes. If the tip lost contact with the pillar, the voltage immediately increased to the compliance limit and the sourced current became negligible.

If the damage during patterning is minimal, the product of the film resistance, R, and the pillar area, A, should be constant. Figure 2 shows the resistance as a function of the inverse area for the patterned film, where each data point represents a resistance measurement on a different pillar. The linear best fit to this data extracts an RA product of 5.4 ± 0.2 Ω μm^2, consistent with independent determinations at Everspin using a CIPT. The intercept of this fit, 194 ± 18 Ω, represents the average series resistance introduced by this probe.

Figure 3 shows a plot of the resistance versus applied magnetic field for a single 200×100 nm^2 pillar. This pillar shows a ΔR of 90 Ω which corresponds to MR=47%, after correcting for the probe series resistance, with a coercivity of 61.5 G and a coupling offset of -60.5 G due to the field produced by the pinned synthetic antiferromagnet (SAF).

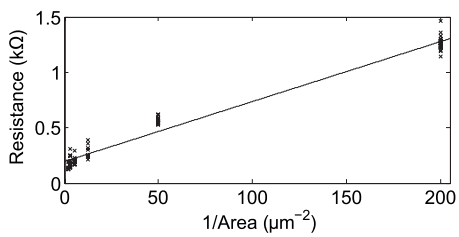

FIG. 2. R vs $1/A$ for 82 pillars using the same probe. The sizes ranged from 1000×500 nm^2 down to 100×50 nm^2. The best linear fit was given by the line with $RA=5.4\pm0.2$ Ω μm^2 and average combined probe and contact resistance of 194 ± 18 Ω. Each size showed moderate resistance variations caused by a combination of contact resistance variation and slight variations in the patterned feature sizes.

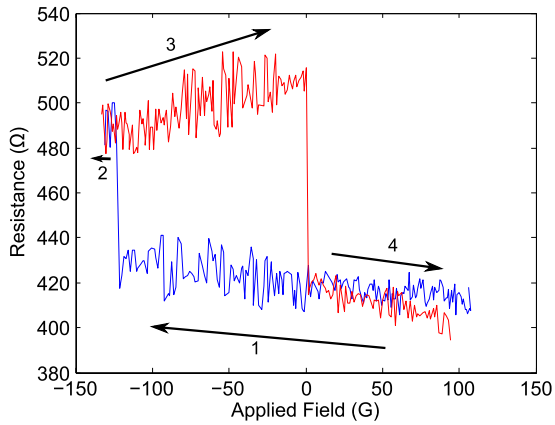

FIG. 3. (Color online) Resistance vs in-plane magnetic field for a 200×100 nm^2 rectangular pillar, having an $H_c\sim61.5$ G and a coupling offset of $H_{cpl}\sim-60.5$ G. The coupling offset was due to the field produced by the pinned SAF beneath the tunnel barrier. A dc current bias of 10 μA with 16.7 ms integrations was used. The sweep started at positive field sweeping down (1, 2) and ended sweeping up (3, 4).

Figure 4 shows current induced switching of the same pillar using current, I, alone. The parallel to antiparallel switch occurred at -3.65×10^6 A/cm^2 and the antiparallel to parallel switch was at $+1.65\times10^6$ A/cm^2. These J_c values are comparable to that expected for a low moment CoFeB alloy at quasistatic time scales.[18] In Fig. 4, the negative slope of the R versus I curves are due to the expected decrease of magnetoresistance with increasing bias voltage.[19] The noise at currents close to zero was due to voltage measurement uncertainty near zero current and the subsequent division of a finite number by nearly zero in the resistance calculation. Comparison between Fig. 3 and Fig. 4 shows the same ΔR at 10 μA, the bias current used in the field sweep, and -12 G, the bias field used in the current sweep, which indicates that the STT reversal volume is the same as that for field reversal. The MR is lower than the $\sim75\%$ expected based on CIPT measurements on the unpatterned film. Given the lack of apparent edge damage in Fig. 2, we conclude this lower MR

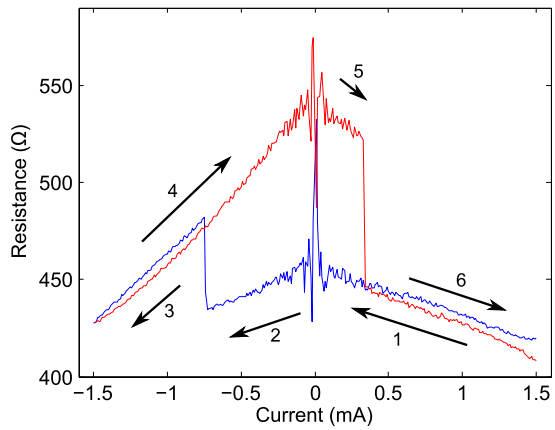

FIG. 4. (Color online) Resistance as a function of current on the same MTJ pillar as in Fig. 3, starting at 1.5 mA sweeping down to -1.5 mA (1, 2, and 3) and then back up to 1.5 mA (4, 5, and 6). The integration time for each voltage measurement was 1.5 ms. A bias field of -12 G was applied to the long axis of the pillar to ensure bistability. The parallel to antiparallel switch occurred at -3.65×10^6 A/cm^2 and the antiparallel to parallel switch occurred at $+1.65\times10^6$ A/cm^2. The sloped sections of the curve where resistance decreased with increasing current magnitude (both polarities) were due to the decrease of magnetoresistance with increasing bias voltage.

is due to difficulty in saturating corners of the rectangular pillars during reversal.

We tested the robustness of the CAFM electrical characterization technique by performing 18 repeated measurements on a single pillar. Between each measurement, the tip was used to check the topography of the pillar, and no changes were observed. The mean value of the probe series resistance was found to be 174 $\Omega \pm 26$ Ω. This variation of the probe series resistance provided separation between the parallel and antiparallel resistance states of approximately four standard deviations for the 200×100 nm^2 pillar examined here.

In summary, we have demonstrated probe-based reading and writing of magnetic tunnel junctions at room temperature using a nonmagnetic probe and spin torque transfer. This work has significant implications for probe-based memory as well as for the metrology of MTJ devices. CAFM tips with a Pt coating provided a sufficiently low contact resistance to distinguish differences in the device resistance and identify switching thresholds. MTJs with a low *RA* product are crucial for patterning into small pillars in order to avoid breakdown before the critical current density is reached. While the smallest pillars investigated here were 100×50 nm^2, the measurement technique should be applicable to reduced pillar sizes, provided that sample drift is controlled. This tool could also be used to study interaction effects between nanopillars.

The authors acknowledge fruitful discussions with Charles Hogg. This work was funded by NSF Grants Nos. ECCS-0507050 and DMR-0804779, U.S.-Israel Binational Science Foundation Grant No. 2006080, and the Carnegie Mellon Data Storage Systems Center.

[1] E. B. Myers, D. C. Ralph, J. A. Katine, R. N. Louie, and R. A. Buhrman, Science **285**, 867 (1999).
[2] G. D. Fuchs, N. C. Emley, I. N. Krivorotov, P. M. Braganca, E. M. Ryan, S. I. Kiselev, J. C. Sankey, D. C. Ralph, R. A. Buhrman, and J. A. Katine, Appl. Phys. Lett. **85**, 1205 (2004).
[3] B. D. Terris and T. Thomson, J. Phys. D: Appl. Phys. **38**, R199 (2005).
[4] M. Sachan, C. Bonnoit, C. Hogg, E. Evarts, J. A. Bain, S. A. Majetich, J. H. Park, and J. G. Zhu, J. Phys. D: Appl. Phys. **41**, 134001 (2008).
[5] P. Vettiger, M. Despont, U. Drechsler, U. Durig, W. Haberle, M. I. Lutwyche, H. E. Rothuizen, R. Stutz, R. Widmer, and G. K. Binnig, IBM J. Res. Dev., **44**, 323 (2000).
[6] W. P. King, T. W. Kenny, K. E. Goodson, G. Cross, M. Despont, U. Durig, H. Rothuizen, G. K. Binnig, and P. Vettiger, Appl. Phys. Lett. **78**, 1300 (2001).
[7] F. S. Teixeira, R. D. Mansano, M. C. Salvadori, M. Cattani, and I. G. Brown, Rev. Sci. Instrum. **78**, 053702 (2007).
[8] E. B. Cooper, S. R. Manalis, H. Fang, H. Dai, K. Matsumoto, S. C. Minne, T. Hunt, and C. F. Quate, Appl. Phys. Lett. **75**, 3566 (1999).
[9] S. F. Lyuksyutov, R. A. Vaia, P. B. Paramonov, S. Juhl, L. Waterhouse, R. M. Ralich, G. Sigalov, and E. Sancaktar, Nature Mater. **2**, 468 (2003).
[10] H. Shin, S. Hong, J. Moon, and J. U. Jeon, Ultramicroscopy **91**, 103 (2002).
[11] J. Y. Son, B. G. Kim, C. H. Kim, and J. H. Cho, Appl. Phys. Lett. **84**, 4971 (2004).
[12] P. Maksymovych, S. Jesse, P. Yu, R. Ramesh, A. P. Baddorf, and S. V. Kalinin, Science **324**, 1421 (2009).
[13] C. Cen, S. Thiel, J. Mannhart, and J. Levy, Science **323**, 1026 (2009).
[14] S. Krause, L. Berbil-Bautista, G. Herzog, M. Bode, and R. Wiesendanger, Science **317**, 1537 (2007).
[15] H. Kubota, Y. Ando, T. Miyazaki, G. Reiss, H. Bruckl, W. Schepper, J. Wecker, and G. Gieres, J. Appl. Phys. **94**, 2028 (2003).
[16] R. W. Dave, G. Steiner, J. M. Slaughter, J. J. Sun, B. Craigo, S. Pietambaram, K. Smith, G. Grynkewich, M. DeHerrera, J. Akerman, and S. Tehrani, IEEE Trans. Magn. **42**, 1935 (2006).
[17] H. Lo and J. A. Bain, *Proceedings of Micro/Nanoscale Heat Transfer Conference (MNHT2008)* (ASME, Tainan, 2008), pp. 52349.
[18] N. D. Rizzo, private communication (July 31, 2009).
[19] G. D. Fuchs, J. A. Katine, S. I. Kiselev, D. Mauri, K. S. Wooley, D. C. Ralph, and R. A. Buhrman, Phys. Rev. Lett. **96**, 186603 (2006).